Mesoporous Materials

DOI: 10.1002/ange.201003270

A Room-Temperature Reactive-Template Route to Mesoporous $ZnGa_2O_4$ with Improved Photocatalytic Activity in Reduction of CO_2**

Shi Cheng Yan, Shu Xin Ouyang, Jun Gao, Ming Yang, Jian Yong Feng, Xiao Xing Fan, Li Juan Wan, Zhao Sheng Li, Jin Hua Ye, Yong Zhou, and Zhi Gang Zou**

Mesoporous materials are of scientific and technological interest due to their potential applications in various areas.[1] Over the past two decades, significant effort has been devoted to the synthesis of mesoporous materials. For instance, mesoporous silica and phosphate metal oxides have been synthesized and applied widely in many industrial processes.[2] However, little progress has been made in the synthesis of mesoporous metal oxides containing more than one type of metal. To date, a limited number of routes including evaporation-induced self-assembly (EISA) and nonaqueous solvent methods have been developed to synthesize multimetallic mesoporous materials such as $Pb_3Nb_4O_{13}$,[3] $Bi_{20}TiO_{32}$,[4] $SrTiO_3$, $MgTa_2O_6$, $Co_xTi_{1-x}O_{2-x}$,[5] and $Ce_{1-x}Zr_xO_2$.[6] In these routes, introducing surfactant molecules or a template is a general method used to construct the mesostructures. Challenges in using the template method to synthesize multimetallic mesoporous materials are uncontrolled phase separation in the multicomponent reactions and poor thermal and chemical stability of the resulting mesoporous structure.[7] Maintaining the complete mesostructure during removal of the template by heating or chemical treatment is a key process for obtaining the expected mesostructures, and increases the uncertainty in a given synthetic route. In addition, to obtain a crystalline mesoporous material, high-temperature heat treatment is usually required for crystallization of the product. However, this process probably induces collapse of mesostructures. Recently, we developed a synthetic route to mesoporous multimetal oxides that uses the inorganic starting reactants directly as pore makers which aid in building the mesoporous structures of multimetal oxides and improve the thermal stability of the resulting mesostructure.[8]

However, in these reported synthetic routes, postcrystallization and introducing or removing an exotemplate are usually needed. In recent years, a route that does not require template removal, which was named "reactive hard templating", was developed to synthesize porous TiN/carbon composite materials.[9] In this route, the template consists of nanostructures of porous graphitic C_3N_4, which thermally decomposes completely during formation of porous TiN. This route provides a means to overcome the problems associated with synthesizing multimetal mesoporous materials. A simplified soft-chemistry route based on a reactive template is expected to allow synthesis to proceed at room temperature without requiring the introduction or removal of a template. Here we report a novel direct method for preparing mesoporous $ZnGa_2O_4$ with a wormhole framework by an ion-exchange reaction at room temperature involving a mesoporous $NaGaO_2$ colloid precursor. The method does not require any additional processes and can be extended to prepare other porous materials, such as $CoGa_2O_4$ and $NiGa_2O_4$.

The X-ray diffraction (XRD) pattern of $NaGaO_2$ powder, which can be indexed as the orthorhombic phase (JCPDS 76-2151), is presented in Figure 1. Scanning electron microscopy (SEM) revealed that the powder particles are irregular in shape with little agglomeration, and most of the particles are larger than 500 nm in diameter (see Supporting Information). The as-prepared $NaGaO_2$ powder can be dispersed in water to form a suspension. When the $NaGaO_2$ suspension is illuminated with a 532 nm laser, a Tyndall effect is observed, that is, the suspension behaves as a colloid (see Supporting Information). Multimodal measurements of particle size distribution by dynamic light scattering show that the $NaGaO_2$ colloidal particles exhibit two peak distributions: 20% of the particles have an average size of 70 nm, and 80% an average size of 335 nm. Most particulate or macroscopic materials in contact with a liquid acquire an electric charge on their surfaces. The zeta potential is an important and useful indicator of this charge that can be used to predict the stability of colloidal suspensions. The zeta potential of $NaGaO_2$ colloidal particles is -21.57 mV (pH 6). This is lower than the critical zeta potential of ± 30 mV for maintaining colloid stability in an aqueous system,[10] that is, the colloidal particles are slightly

[*] S. C. Yan, J. Gao, M. Yang, X. X. Fan, L. J. Wan, Prof. Y. Zhou, Prof. Z. G. Zou
Ecomaterials and Renewable Energy Research Center
National Laboratory of Solid State Microstructures, Nanjing University, 22 Hankou Road, Nanjing 210093 (China)
E-mail: zgzou@nju.edu.cn
J. Y. Feng, Prof. Z. S. Li
Department of Materials Science and Engineering
Nanjing University, 22 Hankou Road, Nanjing 210093 (China)
E-mail: zsli@nju.edu.cn
S. X. Ouyang, Prof. J. H. Ye
Photocatalytic Materials Center (PCMC)
National Institute for Materials Science (NIMS)
Sengen, Tsukuba, Ibaraki 305-0047 (Japan)

[**] This work is supported by the National Basic Research Program of China (No. 2007CB613305), China-Japan cooperation project of science and technology (2009DFA61090) and the National Natural Science Foundation of China (Nos. 50732004 and 20773064)

Supporting information for this article is available on the WWW under http://dx.doi.org/10.1002/anie.201003270.

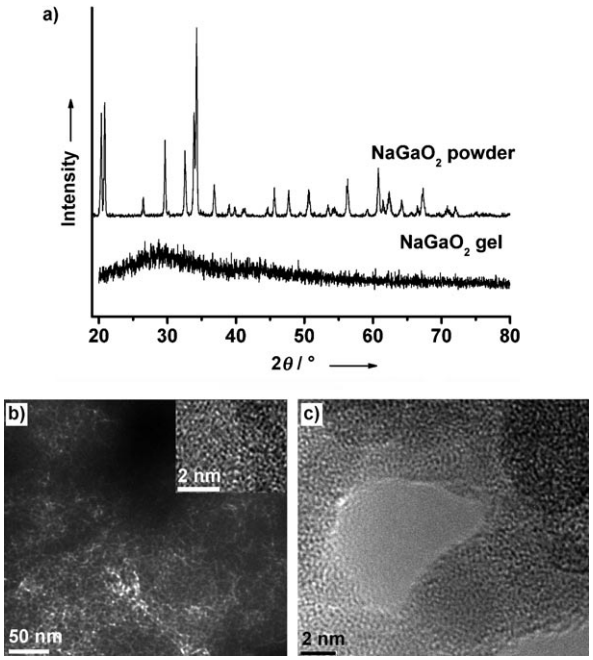

Figure 1. a) XRD patterns of the $NaGaO_2$ powder and gel. b) TEM and HRTEM (inset) images of $NaGaO_2$ colloidal particles. c) High-magnification TEM image of a typical mesopore in the $NaGaO_2$ colloidal particles.

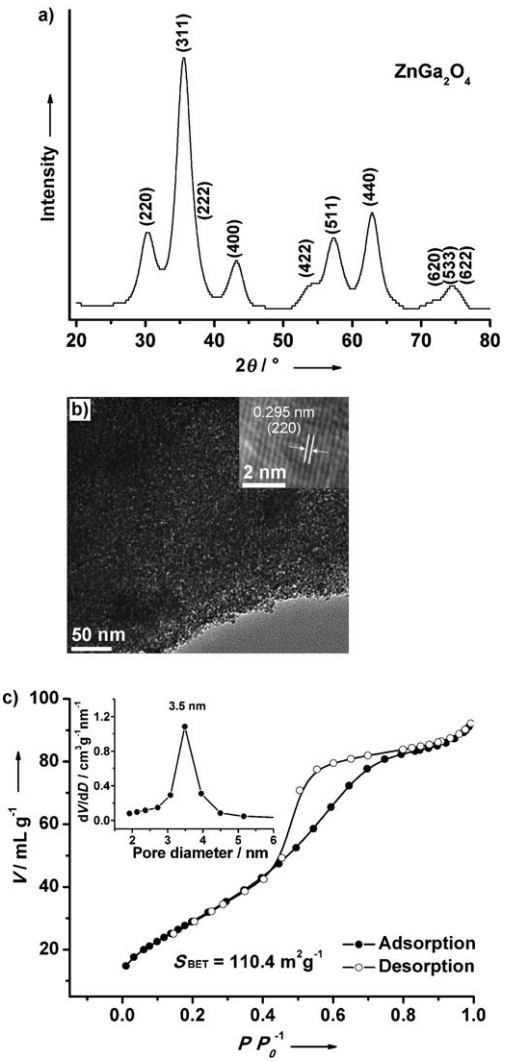

Figure 2. Characterization of meso-$ZnGa_2O_4$. a) XRD pattern. b) TEM image (inset: HRTEM image of the crystal lattice). c) Nitrogen adsorption–desorption isotherms and pore size distribution (inset).

stable and can aggregate easily due to the weak repulsion between them. Upon changing the pH of the $NaGaO_2$ colloidal suspension, the zeta potential became $+42.36$ mV at pH 3 and -32.68 mV at pH 11, that is, the stability of $NaGaO_2$ colloid was improved under both acidic and basic conditions. A gel can be obtained by freeze-drying the $NaGaO_2$ colloidal suspension. An XRD analysis (Figure 1a) indicated that the gel is amorphous, and energy-dispersive X-ray (EDX) analysis showed that the Na/Ga atomic ratio in the gel is close to 0.8:1 (see Supporting Information), probably due to elution of sodium ions from the surface of $NaGaO_2$ colloidal particles. The transmission electron microscopy (TEM) image in Figure 1b shows that the $NaGaO_2$ colloidal particles have a typical mesostructure with a wormhole framework. A high-resolution TEM (HRTEM) image of the mesostructure did not reveal the presence of a crystal lattice (inset of Figure 1b). This implies that the $NaGaO_2$ colloidal particles are amorphous, consistent with the XRD analysis. The mesopores in the colloidal particles can be observed at high magnification (Figure 1c).

To understand the ion exchange between $NaGaO_2$ colloidal suspension and an aqueous solution of $Zn(CH_3COO)_2$, in situ observations were performed with an optical microscope. When the $NaGaO_2$ colloidal suspension was left undisturbed under ambient conditions for an extended period, a mesh of aggregated colloidal particles formed on the micrometer scale due to the low stability of the colloid (see Supporting Information). An in situ ion-exchange reaction on the amorphous $NaGaO_2$ framework could be observed when Zn^{2+} ions were introduced into the reaction system. As illustrated in Figure 2a, the XRD pattern of the product from the ion-exchange reaction can be indexed as cubic spinel $ZnGa_2O_4$ (denoted meso-$ZnGa_2O_4$) with a cell parameter of $a = 8.335$ Å, which is in good agreement with JCPDS 38-1240. The composition of the as-prepared $ZnGa_2O_4$ was further confirmed by EDX analysis (see Supporting Information). The diffraction peaks in the XRD pattern of meso-$ZnGa_2O_4$ are clearly broadened. From the XRD data, the grain size was estimated by the Scherrer formula to be about 5 nm. Usually, soft-chemical routes performed at room-temperature, such as co-precipitation, produce amorphous $ZnGa_2O_4$.[11] In this case, the ion-exchange process occurs by a unique reaction between a weakly acidic $Zn(CH_3COO)_2$ (pH 6) solution and an alkalescent $NaGaO_2$ (pH 8) colloidal suspension. Aggregation of $ZnGa_2O_4$ depends strongly on the Zn-containing precursor. In this reaction, the strong electrolyte $Zn(NO_3)_2$ instead of the weak electrolyte $Zn(CH_3COO)_2$ will produce amorphous $ZnGa_2O_4$. This is probably due to the faster reaction rate between $Zn(NO_3)_2$ and $NaGaO_2$ than between $Zn(CH_3COO)_2$ and $NaGaO_2$. This fact may support the argu-

ment that the reaction rate between $Zn(CH_3COO)_2$ and $NaGaO_2$ is appropriate for nucleating and growing crystalline $ZnGa_2O_4$. The TEM images show that meso-$ZnGa_2O_4$ also has a wormhole framework like the $NaGaO_2$ colloidal particles (Figure 2b). Apparently, the mesostructure of $ZnGa_2O_4$ resulted from agglomeration of nanoparticles. An HRTEM analysis indicates that the lattice spacing is 0.295 nm for the (220) plane, which provides further evidence that the product is crystalline $ZnGa_2O_4$. Nitrogen adsorption–desorption studies on as-prepared meso-$ZnGa_2O_4$ showed a type IV isotherm, typical of mesoporous materials (Figure 2c). The pore diameter calculated from the nitrogen adsorption isotherm by the Barrett–Joyner–Halenda (BJH) method is 3.5 nm, and the specific surface area calculated from the linear region of the Brunauer–Emmett–Teller (BET) plot ranging from $P/P_0 = 0.05$ to $P/P_0 = 0.15$ is 110.4 $m^2 g^{-1}$.

It is interesting to discover a formation mechanism of mesopores that does not require introducing a template or surfactant molecules. As illustrated in Figure 3, it seems reasonable to speculate that the $NaGaO_2$ powder dispersed in

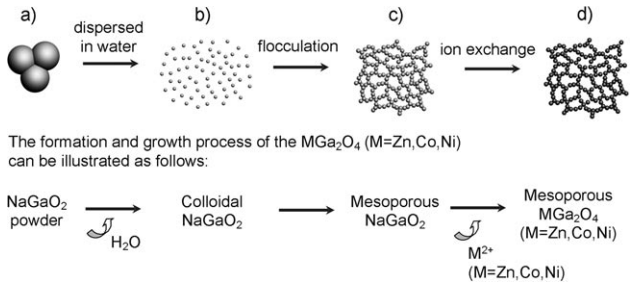

Figure 3. Illustration of the formation of a mesoporous colloidal template and an ion-exchange reaction based on the colloidal template. a) $NaGaO_2$ solid powder particles. b) $NaGaO_2$ colloidal particles obtained by dispersing the $NaGaO_2$ powders in deionized water. c) Formation of a mesoporous $NaGaO_2$ colloidal template by flocculation. d) Formation of mesoporous $ZnGa_2O_4$ by ion-exchange reaction on the $NaGaO_2$ colloidal template.

water can form amorphous colloidal particles, which tend to form the mesoporous $NaGaO_2$ colloid by flocculation due to the weak repulsion between the colloidal particles. The ion-exchange process between Zn^{2+} and Na^+ is expected to be due to the $NaGaO_2$ mesoporous framework, because $ZnGa_2O_4$ crystal particles could nucleate and grow there. The mesoporous structure of the $NaGaO_2$ colloid is maintained in the generated $ZnGa_2O_4$ after ion exchange, probably because the reaction rate is moderate. For the $ZnGa_2O_4$ particles suspended in water, a high zeta potential of +52.66 mV was measured. The opposite sign of the charge of zeta potential for the $ZnGa_2O_4$ particles and $NaGaO_2$ colloidal particles suggests that the particles attract each other. This would be beneficial for maintaining the $NaGaO_2$ mesoporous framework during the ion-exchange reaction. Moreover, changes to the pores in $NaGaO_2$ may take place during phase transformation due to a change in crystal structure. However, the porous structure of $NaGaO_2$ colloid can compensate for the volume change by tuning the pore size. This may promote the mesostructure of $NaGaO_2$ being inherited by $ZnGa_2O_4$.

The route reported here is applicable to preparation of other mesoporous spinel AB_2O_4-type oxides. Mesoporous $CoGa_2O_4$ and $NiGa_2O_4$ were synthesized by this method. Unlike $ZnGa_2O_4$, the MGa_2O_4 (M = Co, Ni) samples obtained by ion exchange at room temperature are amorphous. The specific surface areas of amorphous $NiGa_2O_4$ and $CoGa_2O_4$ are 363.3 and 202.3 $m^2 g^{-1}$, respectively. The samples exhibited a uniform pore size distribution. TEM observations (see Supporting Information) showed that the wormholes in these amorphous products are similar to those in the $NaGaO_2$ colloid due to the amorphous phase transformation with slight particle growth. By hydrothermal treatment of these amorphous samples at 180 °C for 5 h, crystalline mesoporous $CoGa_2O_4$ and $NiGa_2O_4$ can be obtained. Compared with the amorphous products, the specific surface areas of crystalline $CoGa_2O_4$ and $NiGa_2O_4$ decreased to 82.7 and 87.1 $m^2 g^{-1}$, respectively. The pore sizes of crystalline mesoporous $CoGa_2O_4$ and $NiGa_2O_4$ exhibit bimodal distributions (Figure 4), and the average values of the pore diameter were 2.5 and 8 nm, respectively. The grain size of crystalline $CoGa_2O_4$ and $NiGa_2O_4$ is about 10 nm (see Supporting Information). Therefore, the results of these experiments indicate that amorphous MGa_2O_4 (M = Co, Ni) can form rapidly at room temperature, and that subsequent hydrothermal treatment induces crystallization and growth of the amorphous particles. The mesopores in $CoGa_2O_4$ and $NiGa_2O_4$ are formed by agglomeration of nanoparticles, similar to meso-$ZnGa_2O_4$. Compared with amorphous $CoGa_2O_4$ and $NiGa_2O_4$, the bimodal pore size distribution and low BET surface area of crystalline $CoGa_2O_4$ and $NiGa_2O_4$ can be attributed to grain growth during hydrothermal treatment.

AB_2O_4-type oxides with spinel structure have potential applications in many fields such as catalysis, gas sensors, and photoelectronics. In particular, $ZnGa_2O_4$ is a transparent and conductive material which should be useful for UV photoelectronic devices.[12] $ZnGa_2O_4$ also shows potential as a photocatalyst for wastewater treatment and hydrogen production by water splitting.[13,14] Here meso-$ZnGa_2O_4$ was used as a photocatalyst to convert CO_2 into methane (CH_4) under irradiation of UV light.

Carbon dioxide, which is released mainly by burning of fossil fuels, is the primary cause of global warming. Converting CO_2 into valuable hydrocarbons by means of solar energy is one of the best solutions to both global warming and energy shortage. Generally, CO_2 can be photoreduced to CH_4 in the presence of water vapor by using a wide band gap semiconductor such as TiO_2 as photocatalyst. The photogenerated holes in the valence band oxidize water to generate hydrogen ions by the reaction $H_2O \rightarrow 1/2\,O_2 + 2\,H^+ + 2\,e^-$ ($E^o_{redox} = 0.82$ V vs. NHE). The photogenerated electrons in the conduction band reduce CO_2 to CH_4 by the reaction $CO_2 + 8\,e^- + 8\,H^+ \rightarrow CH_4 + 2\,H_2O$ ($E^o_{redox} = -0.24$ V vs. NHE).[15] The electronic structure of $ZnGa_2O_4$ has been calculated by using plane-wave-based density functional theory.[14] The valence band was mainly composed of the O 2p orbitals, whereas the conduction band was formed by hybridization of Ga 4s4p and Zn 4s4p orbitals. The band gap of the as-prepared $ZnGa_2O_4$ was determined from the UV/Vis

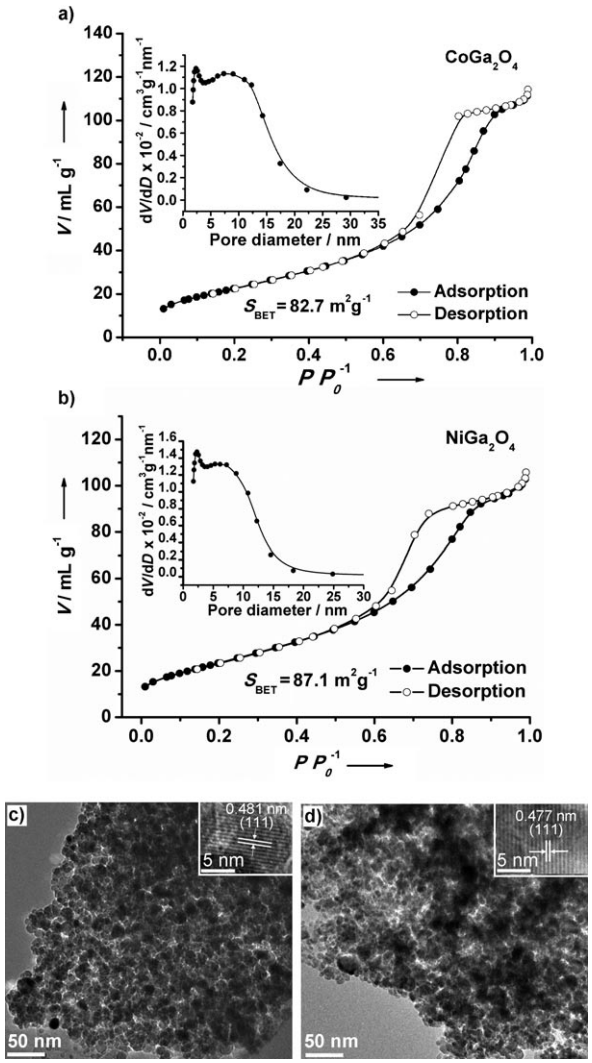

Figure 4. Nitrogen absorption–desorption isotherms, pore size distribution (inset), TEM images, and HRTEM images of the lattice (inset) for a, c) $CoGa_2O_4$ and b, d) $NiGa_2O_4$ obtained by hydrothermal treatment of amorphous MGa_2O_4 (M = Co, Ni) samples, prepared by ion exchange at room temperature.

absorption spectrum to be 4.4 eV (see Supporting Information). The position of the conduction and valence bands in as-prepared $ZnGa_2O_4$ was determined by the following equation: $E_{CB} = X - E_c - 0.5\,E_g$, where E_c is the energy of free electrons on the hydrogen scale (4.5 eV), X is the electronegativity of the semiconductor, and E_g is the band-gap energy of the semiconductor. The edge of the valence band E_{VB} of $ZnGa_2O_4$ was determined to be 3.13 V versus NHE, which is more positive than $E^o(H_2O/H^+)$ (0.82 V vs. NHE). The edge of the conduction band was estimated to be −1.27 V versus NHE, which is more negative than $E^o(CO_2/CH_4)$(−0.24 V vs. NHE). This indicates that the electrons and holes photogenerated on irradiation of $ZnGa_2O_4$ can react with adsorbed CO_2 and H_2O to produce CH_4. Figure 5 shows that meso-$ZnGa_2O_4$ (CH_4: 5.3 ppm h^{-1}) exhibits higher activity than $ZnGa_2O_4$ (CH_4: trace) obtained by solid-state reaction of ZnO and Ga_2O_3 at 1100 °C for 16 h (denoted ss-$ZnGa_2O_4$). This is related to strong gas adsorption by the

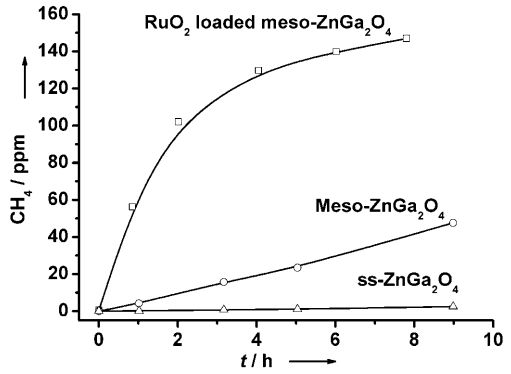

Figure 5. CH_4 generation over various $ZnGa_2O_4$ samples as a function of irradiation time.

mesostructure and more reaction sites arising from high specific surface area ($S_{BET} = 110.4\ m^2 g^{-1}$ for meso-$ZnGa_2O_4$ and 4.6 $m^2 g^{-1}$ for ss-$ZnGa_2O_4$). The generation rate of CH_4 over meso-$ZnGa_2O_4$ could be significantly enhanced by loading 1 wt % RuO_2 as co-catalyst to improve separation of the photogenerated electron–hole pairs (CH_4: 50.4 ppm h^{-1}), as demonstrated in photocatalytic water splitting.[14]

In summary, a reactive templating route to preparing mesoporous $ZnGa_2O_4$ at room temperature has been reported. The reaction pathway involves an ion-exchange process with a porous $NaGaO_2$ colloidal template as the precursor. The route is effective for synthesizing porous AB_2O_4-type materials by a simple method. By using RuO_2 as co-catalyst, the as-prepared mesoporous $ZnGa_2O_4$ shows high photocatalytic activity for converting CO_2 into CH_4 under light irradiation, because of strong gas adsorption and large specific surface area of the mesoporous photocatalyst. Mesoporous $ZnGa_2O_4$ is potentially an effective photocatalyst for the photoreduction of CO_2.

Experimental Section

$NaGaO_2$ solid powders were prepared by heating a stoichiometric mixture of Na_2CO_3 and Ga_2O_3 at 850 °C for 12 h. Mesoporous $ZnGa_2O_4$ was prepared as follows: $NaGaO_2$ colloidal suspension (0.2 mol L^{-1}, 10 mL) was added to an aqueous solution of Zn$(CH_3COO)_2$ (0.05 mol L^{-1}, 20 mL) and the mixture stirred for 3 h at room temperature to form mesoporous $ZnGa_2O_4$. The sediment was separated by centrifugation and dried at 60 °C for 2 h.

Mesoporous $CoGa_2O_4$ and $NiGa_2O_4$ were synthesized by a similar procedure. $NaGaO_2$ colloidal suspension (0.2 mol L^{-1}, 10 mL) was added to an aqueous solution of $CoSO_4$ or Ni$(CH_3COO)_2$ (0.05 mol L^{-1}, 20 mL) and the mixture stirred for 1 h. The mixture was then heated in a Teflon-lined hydrothermal autoclave at 180 °C for 5 h to form mesoporous crystalline $CoGa_2O_4$ or $NiGa_2O_4$.

The crystalline phases of these as-prepared products were determined by powder XRD (Rigaku Ultima III, CuKa radiation). The size, size distribution, and zeta potential of $NaGaO_2$ colloidal particles were determined by a zeta potential analyzer (Zeta PALS, Brookhaven Instruments Co., USA). The specific surface area of the samples was measured by nitrogen sorption at 77 K on a surface area and porosity analyzer (Micromeritics TriStar 3000, USA) and calculated by the BET method. The morphology of the samples was observed by TEM (FEI Tecnai G2 F30 S-Twin, USA).

In the photocatalytic reduction of CO_2, $ZnGa_2O_4$ powder (0.1 g) was uniformly dispersed on a glass reactor with an area of 4.2 cm^2. A

300 W Xenon arc lamp was used as the light source for the photocatalytic reaction. The volume of the reaction system was about 230 mL. The reaction setup was vacuum-treated several times, and then high-purity CO_2 gas was introduced into the reaction to achieve ambient pressure. Deionized water (0.4 mL) was injected into the reaction system as reducing agent. During the irradiation, about 1 mL of gas was taken from the reaction cell at given intervals for subsequent CH_4 concentration analysis with a gas chromatograph (GC-14B, Shimadzu Corp., Japan).

Received: May 30, 2010
Published online: July 22, 2010

Keywords: ion exchange · mesoporous materials · photochemistry · reduction · template synthesis

[1] a) A. Navrotsky, O. Trofymluk, A. Levchenko, *Chem. Rev.* **2009**, *109*, 3885; b) Y. Ren, L. J. Hardwick, P. G. Bruce, *Angew. Chem.* **2010**, *122*, 2624; *Angew. Chem. Int. Ed.* **2010**, *49*, 2570; c) X. M. Jiang, T. L. Ward, Y. S. Cheng, J. W. Liu, C. J. Brinker, *Chem. Commun.* **2010**, *46*, 3019; d) R. Liu, D. Wu, X. Feng, K. Mullen, *Angew. Chem.* **2010**, *122*, 2619; *Angew. Chem. Int. Ed.* **2010**, *49*, 2565.

[2] a) Y. Wan, D. Y. Zhao, *Chem. Rev.* **2007**, *107*, 2821; b) D. Y. Zhao, J. L. Feng, Q. S. Huo, N. Melosh, G. H. Fredrickson, B. F. Chmelka, G. D. Stucky, *Science* **1998**, *279*, 548; c) J. Sun, C. Bonneau, Á. Cantín, A. Corma, M. J. Díaz-Cabañas, M. Moliner, D. Zhang, M. Li, X. Zou, *Nature* **2009**, *458*, 1154.

[3] X. Fan, J. Gao, Y. Wang, Z. Li, Z. Zou, *J. Mater. Chem.* **2010**, *20*, 2865.

[4] L. D. Kong, H. H. Chen, W. M. Hua, S. C. Zhang, J. M. Chen, *Chem. Commun.* **2008**, *40*, 4977.

[5] D. Grosso, C. Boissiere, B. Smarsly, T. Brezesinski, N. Pinna, P. A. Albouy, H. Amenitsch, M. Antonietti, C. Sanchez, *Nat. Mater.* **2004**, *3*, 787.

[6] Q. Yuan, Q. Liu, W. G. Song, W. Feng, W. L. Pu, L. D. Sun, Y. W. Zhang, C. H. Yan, *J. Am. Chem. Soc.* **2007**, *129*, 6698.

[7] a) D. Grosso, C. Boissiere, L. Nicole, C. Sanchez, *J. Sol-Gel Sci. Technol.* **2006**, *40*, 141; b) Y. Narendar, G. L. Messing, *Catal. Today* **1997**, *35*, 247.

[8] X. Fan, Y. Wang, X. Chen, L. Gao, W. Luo, Y. Yuan, Z. Li, T. Yu, J. Zhu, Z. Zou, *Chem. Mater.* **2010**, *22*, 1276.

[9] a) A. Fischer, Y. S. Jun, A. Thomas, M. Antonietti, *Chem. Mater.* **2008**, *20*, 7383; b) Y. S. Jun, W. H. Hong, M. Antonietti, A. Thomas, *Adv. Mater.* **2009**, *21*, 4270.

[10] Zeta potential of colloids in water and waste water, ASTM Standard D 4187-82, American Society for Testing and Materials, **1985**.

[11] H. K. Jung, D. S. Park, Y. C. Park, *Mater. Res. Bull.* **1999**, *34*, 43.

[12] T. Omata, N. Ueda, K. Ueda, H. Kawazoe, *Appl. Phys. Lett.* **1994**, *64*, 1077.

[13] X. Chen, H. Xue Z. H. Li, L. Wu, X. X. Wang, X. Z. Fu, *J. Phys. Chem. C* **2008**, *112*, 20393.

[14] K. Ikarashi, J. Sato, H. Kobayashi, N. Saito, H. Nishiyama, Y. Inoue, *J. Phys. Chem. B* **2002**, *106*, 9048.

[15] V. P. Indrakanti, J. D. Kubicki, H. H. Schobert, *Energy Environ. Sci.* **2009**, *2*, 745.

